Journal of Superconductivity, Vol. 7, No. 3, 1994

Normal-State Transport Properties of Fullerene Superconductors

A. Zettl,[1] Li Lu,[1] X.-D. Xiang,[1] J. G. Hou,[1] W. A. Vareka,[1] and M. S. Fuhrer[1]

Received 31 July 1993

The normal-state transport properties of alkali-metal-doped fullerene crystals are explored. The Hall effect has been measured in K_xC_{60} from room temperature to T_c. The electrical resistivity ρ for K_3C_{60} and Rb_3C_{60} has been measured over a wide temperature range (20–650 K), and notable differences are observed for the materials at both low and high temperatures. The electrical resistivity of Rb_3C_{60} has been measured in hydrostatic pressures up to 9 kbar. The resistivity is highly pressure sensitive. The transport results give an insight into the normal-state conduction mechanism and thus have consequences for the superconductivity mechanism.

KEY WORDS: Alkali-metal-doped fullerenes; normal-state transport; superconductivity.

1. INTRODUCTION

The normal-state properties of a superconductor are often invaluable in establishing parameters directly relevant to the superconducting state. For example, in a BCS phonon superconductor, the transport electron–phonon coupling constant extracted from the normal-state electrical resistivity is often a good approximation to the electron–phonon coupling strength λ which dictates T_c. Signatures of an exotic superconductivity mechanism may be revealed by normal-state carrier sign and number, or unusual temperature and pressure-dependent scattering. Although some normal-state transport data exist for the alkali-metal-doped fullerene superconductors, the normal state has not been fully characterized. Here we explore the Hall effect, the high- and low-temperature electrical resistivity, and pressure-dependent transport in M_xC_{60}, where M is either K or Rb.

2. SAMPLE PREPARATION

Single crystals of pure C_{60} were first produced by vapor transport. Appropriate electrical leads were then attached to the samples, and the specimens were subjected to alkali metal vapor at elevated temperature. The degree of sample doping was monitored via the sample electrical resistance [1].

Figure 1 shows the electrical resistivity $\rho(T)$ of K_xC_{60} for four different fixed doping levels. The upper

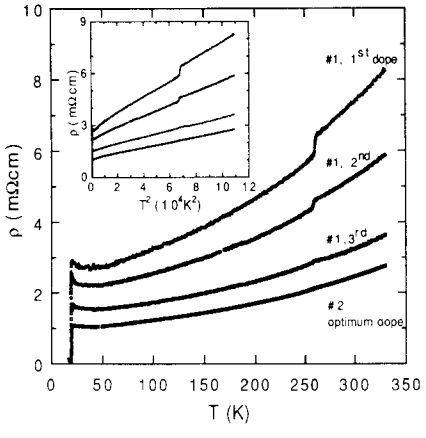

Fig. 1. $\rho(T)$ for K_xC_{60} at various doping levels. The bottom curve corresponds to near-optimum doping, with $x = 3$. Inset: Same data plotted versus T^2. Note that the curves in the inset all extrapolate to the same point on the T^2 axis outside the left frame, indicating that the general form of the apparent resistivity at different doping levels is $\rho = \gamma(\rho_0 + \alpha T^2)$; only γ is doping dependent and represents the volume fraction of K_3C_{60} within the specimen.

[1]Department of Physics, University of California at Berkeley, and Materials Sciences Division, Lawrence Berkeley Laboratory, Berkeley, California 94720.

0896-1107/94/0600-0639$07.00/0

three curves in the main body of the figure are for a given C_{60} crystal at three different fixed *average* values of potassium concentration x, all presumably with $x<3$. As x increases in K_xC_{60}, the overall resistivity decreases, and the anomaly at 260 K (associated with the remaining pristine regions of C_{60} in the specimen undergoing a rotational ordering transition and hence inducing a strain field on the conducting K_3C_{60} channels) decreases accordingly. The bottom curve corresponds to another crystal which we infer is doped near the optimum value of $x=3$ since it is close to the resistivity minimum for the K_xC_{60} system. The inset to the figure shows that at all doping levels, a T^2 functional form for $\rho(T)$ is observed. Indeed, aside from the 260 K anomaly, all the data of Fig. 1 differ only by a geometrical scale factor. This argues strongly that underdoped K_xC_{60} consists of line-phase islands of K_3C_{60} in a pure C_{60} matrix, as has been previously proposed.

3. HALL EFFECT

Figure 2 shows the Hall coefficient for K_xC_{60} at three different doping levels. A variable doping level changes the apparent carrier concentration, which we again interpret as an effective geometry effect. The solid squares are the most relevant data and correspond to near-optimally-doped K_3C_{60}. The dashed line in Fig. 2a corresponds to a carrier concentration of 3 electrons per C_{60} molecule. Hence, near room temperature K_3C_{60} has a carrier concentration of $3e^-/C_{60}$. This suggests that all the alkali-donated electrons are mobile. The Hall coefficient is temperature dependent, changing by a factor of 2 between room temperature and T_c. The origin of this modest temperature dependence is not yet clear, but it may represent a freeze-out of carriers at lower temperature due to correlation-induced localization, or reflect a multi-band electronic structure.

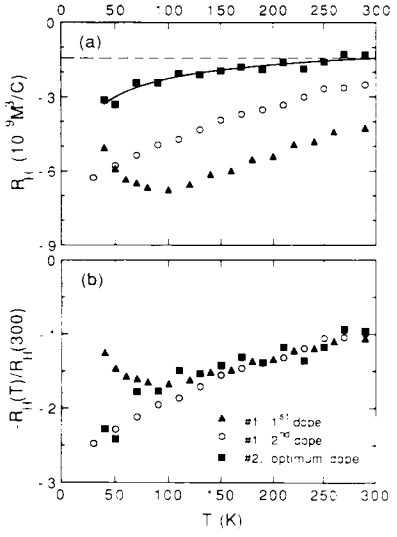

Fig. 2. Temperature dependence of Hall coefficient in K_3C_{60}. The solid squares correspond to K_3C_{60}. The dashed line in (a) represents three electrons per C_{60} molecule. In (b), the data have been normalized to the room-temperature values.

4. TEMPERATURE-DEPENDENT RESISTIVITY

Previous studies [1,2] have shown that over a rather broad temperature range, both K_3C_{60} and Rb_3C_{60} display a similar T^2-like temperature dependent resistivity when the specimen is measured at constant pressure (typically 1 atm). The absolute value of the resistivity of Rb_3C_{60} exceeds that of K_3C_{60} by about a factor of 2 (over a broad temperature range), and both materials in single crystal form typically have a residual resistivity ratio equal to 2. However, at both low and high temperatures, the $\rho(T)$ curves for K_3C_{60} and Rb_3C_{60} differ significantly.

Figure 3 shows the normalized $\rho(T)$ for K_3C_{60} and Rb_3C_{60} plotted versus reduced temperature T/T_c. Between T_c and $3T_c$, K_3C_{60} is well fitted by a power law, with T^7 providing the best fit (a more conventional T^5 curve is also shown for comparison). We do not attribute any particular significance to the

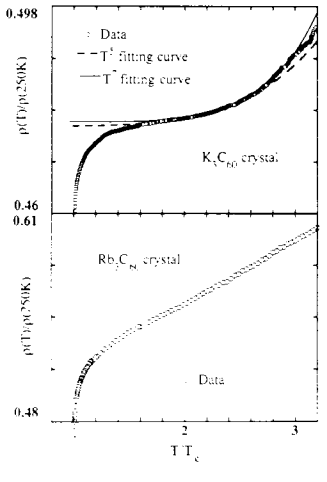

Fig. 3. Constant pressure $\rho(T)$ data for K_3C_{60} and Rb_3C_{60} at low temperatures ($<3T_c$).

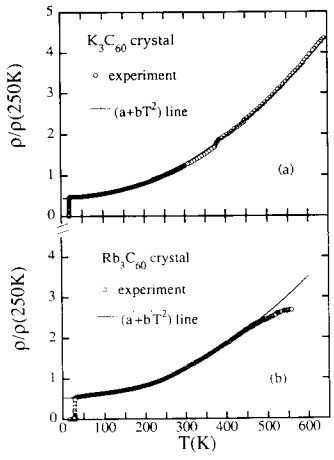

Fig. 4. Normalized constant pressure $\rho(T)$ data from T_c to high temperatures for K_3C_{60} and Rb_3C_{60}; the solid lines are T^2 fitting curves. Note the resistivity saturation in Rb_3C_{60} above 500 K.

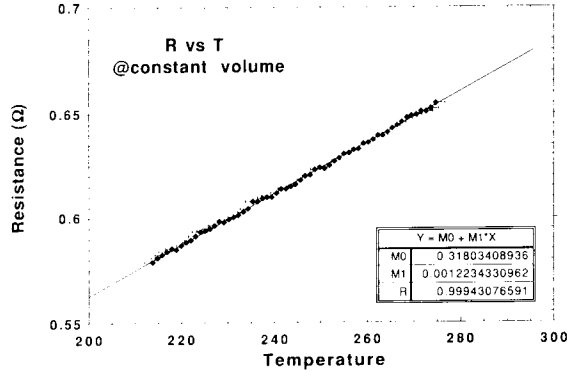

Fig. 5. Constant-volume $\rho(T)$ in Rb_3C_{60} over a limited temperature range. The data do not fit a T^2 law. The solid line represents linear-T behavior.

exponent. Rb_3C_{60}, on the other hand, is adequately fitted by a linear temperature dependence. Since the two materials have similar coefficients of thermal expansion, the differences in $\rho(T)$ may reflect alkali optic mode contributions to the carrier scattering in this temperature regime.

Figure 4 shows the temperature-dependent resistivities over a very broad temperature range. In K_3C_{60}, $\rho(T)$ follows a T^2 law up to the highest measured temperature, 650 K. The small anomaly near 380 K may be due to a structural phase transition or phase separation transition [3] in the material. No evidence of high-temperature resistivity saturation is observed, consistent with high-temperature resistance studies of thin films [4]. Rb_3C_{60}, on the other hand, shows a clear deviation from the T^2 law starting around 500 K. The resistivity tends to saturate above this temperature, which we interpret as evidence that the mean free path is approaching a characteristic intrinsic length scale in the material. Using an absolute value for the resistivity deduced from fluctuation conductivity experiments [2], we find that the relevant intrinsic length scale is roughly the on-ball C–C distance (as opposed to the lattice constant of Rb_3C_{60}). This suggests on-ball (phonon) scattering at high temperatures in this system. By analogy, we expect the resistivity of K_3C_{60} to saturate above about 700 K; this prediction has not yet been tested.

5. PRESSURE EFFECTS ON THE RESISTIVITY

Most theoretical predictions for transport coefficients assume a constant volume for the crystal. However, typical transport measurements are performed under constant pressure conditions. The T^2-like temperature dependence of $\rho(T)$ described above may in fact not reflect the true constant-volume behavior of $\rho(T)$. In an earlier study [5], the constant pressure data for $\rho(T)$ in K_3C_{60} were converted to "constant volume" values using a temperature-dependent density of states correction; a T^2 law was no longer observed. Here we explore $\rho(T, V, P)$ in Rb_3C_{60} where external hydrostatic pressure P can be applied to keep the sample volume V constant.

A conventional Teflon-seal pressure cell was employed to measure $\rho(T, P, V=\text{const})$ in Rb_3C_{60} crystals. Figure 5 shows preliminary data over a restricted temperature range. Over this temperature range, the natural pressure drop in the pressure cell with decreasing temperature compensates precisely for the thermal contraction of the crystal with decreasing temperature; hence the sample volume remains constant. The average applied pressure is about 5 kbar. Figure 5 indicates that these constant-volume data might be better described as linear, rather than T^2. Data over a wider temperature and pressure range are needed to drawn any firm conclusions.

The absolute value of the resistivity in Rb_3C_{60} is found to be extremely pressure dependent. In fact, if a pressure of 9 kbar is applied to Rb_3C_{60} at room temperature, the resistivity is reduced to a value *below* the residual resistivity (determined at 1 bar pressure and low temperatures). This suggests that the residual resistivity is not just a chemical impurity effect, but most probably due to pressure-dependent structural disorder.

Figure 6 shows at fixed temperature the $\rho(P)$ behavior for Rb_3C_{60}. The data are well fitted by an

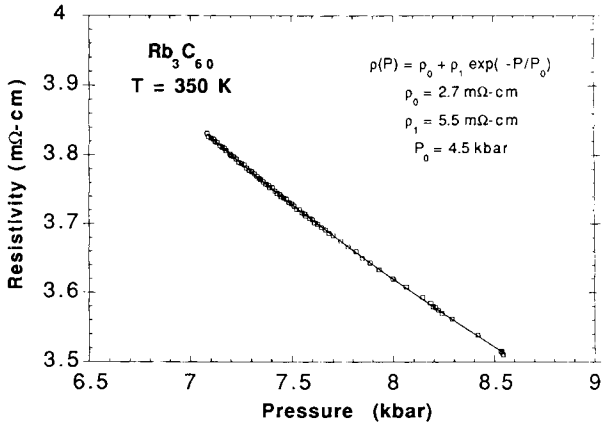

Fig. 6. Pressure dependence of the electrical resistivity in Rb_3C_{60} at 350 K. The solid line is an exponential dependence with fitting parameters given on the figure.

exponential form. $\rho(P)$ has also been measured at room temperature, and a similar functional form is found, with a similar "activation" pressure $P_0 =$ 4.5 kbar. The exponential dependence of ρ on pressure may have implications for the normal-state conduction mechanism, in that the primary consequence of increased pressure may be to decrease the C_{60} ball-to-ball distance. A tunneling type of conduction mechanism between balls comes to mind.

6. CONCLUSIONS

In K_3C_{60} the free carriers are electrons in a concentration corresponding roughly to three per C_{60} molecule. The electrical resistivity measured at constant pressure follows a near-perfect T^2 law up to 650 K in K_3C_{60}, while resistivity saturation is observed in Rb_3C_{60} above 500 K. Pressure studies in Rb_3C_{60} show an exponential pressure dependence of the normal-state resistivity, and that the constant-volume temperature-dependent resistivity deviates significantly from a T^2 law.

ACKNOWLEDGMENTS

We thank Brian Burk, Gabriel Briceno, Vincent Crespi, and Marvin L. Cohen for helpful interactions. This work was supported by the Office of Energy Research, Office of Basic Energy Sciences, Materials Sciences Division of the U.S. Department of Energy under contract DE-AC03-76SF00098. F. S. Fuhrer acknowledges support from an NSF Fellowship.

REFERENCES

1. X.-D. Xiang, J. G. Hou, G. Briceño, W. A. Vareka, R. Mostovoy, A. Zettl, V. H. Crespi, and M. L. Cohen, *Science* **256**, 1190 (1992).
2. X.-D. Xiang, J. G. Hou, A. Zettl, V. H. Crespi, and M. L. Cohen, *Nature (London)* **361**, 54 (1993).
3. D. M. Poirier and J. H. Weaver, *Phys. Rev. B* **47**, 10959 (1993).
4. A. F. Hebard, private communication.
5. Vincent H. Crespi, J. H. Hou, X.-D. Xiang, Marvin L. Cohen, and A. Zettl, *Phys. Rev. B* **46**, 12064 (1992).